Influence of dielectric substrate on the responsivity of microstrip dipole-antenna-coupled infrared microbolometers

Iulian Codreanu and Glenn D. Boreman

We report on the influence of the dielectric substrate on the performance of microstrip dipole-antenna-coupled microbolometers. The location, the width, and the magnitude of the resonance of a printed dipole are altered when the dielectric substrate is backed by a ground plane. A thicker dielectric substrate shifts the antenna resonance toward shorter dipole lengths and leads to a stronger and slower detector response. The incorporation of an air layer into the antenna substrate further increases thermal impedance, leading to an even stronger response and shifting the antenna resonance toward longer dipole lengths. © 2002 Optical Society of America

OCIS codes: 040.0040, 040.3060, 230.5750, 220.3740, 220.4000, 230.5440.

1. Introduction

A variety of infrared (IR) spectroscopic and imaging applications require fast detectors. Since the response time of a thermal detector is proportional to its volume, it seems reasonable to reduce the detector volume until the desired time constant is attained. However, as the detector dimensions are reduced, its ability to collect radiation decreases, adversely affecting its responsivity. One way of maintaining a reasonable responsivity, while obtaining a fast response, is to integrate the detector with an antenna. When this is done, the radiation-collection function is separated from the radiation-detection function. The antenna collects the radiation and generates an oscillating optical-frequency electric field at its terminals. This oscillating field is detected by a square-law sensor. For efficient energy transfer, proper matching between the sensor and the antenna must be ensured. In general the antenna is a metallic structure whose size is comparable with the wavelength of the radiation being detected. The sensor (bolometer, metal–oxide–metal diode, and so on) dimension is a small fraction of the wavelength. A sensor can be integrated with various types of antennas[1–4] to achieve desired spectral, polarization, and angular response characteristics.

Microstrip antennas are widely used in the microwave spectral region.[5] They are easy to fabricate by use of standard integrated-circuit techniques, have low profile, are conformal, and can be easily integrated in arrays and with electronic components. Microstrip antennas are broadside and narrow band. Low gain is the major drawback of the microstrip antennas. A microstrip antenna consists of a thin metal patch placed on a dielectric substrate backed by a ground plane. A side view of a microstrip patch antenna is shown in Fig. 1. The length of the metallic patch, L, is slightly shorter than half the wavelength of the incident radiation scaled to the index of refraction of the dielectric substrate. A plane wave is normally incident on the antenna structure; the electric field of the incident wave is parallel to the microstrip patch. The interaction of the antenna with the incident radiation occurs mainly at the edges of the patch, where the incident radiation induces an electric field between the edge of the metal and the ground plane. The TM guided waves launched at the ends of the patch generate a standing-wave pattern. The electric field distribution has a null at the center of the patch and reaches its maximum at the edges of the patch. The antenna magnetic field has a maximum at the center of the patch. Electric currents of equal magnitude and opposite propagation directions are induced on the bottom of the patch and on the top of the ground plane. At resonance, the induced current is strongest at the

The authors are with the School of Optics and Center for Research and Education in Optics and Lasers, University of Central Florida, P.O. Box 162700, Orlando, Florida 32816-2700. G. Boreman's e-mail address is boreman@creol.ucf.edu.

Received 25 September 2001; revised manuscript received 2 January 2002.

0003-6935/02/101835-06$15.00/0

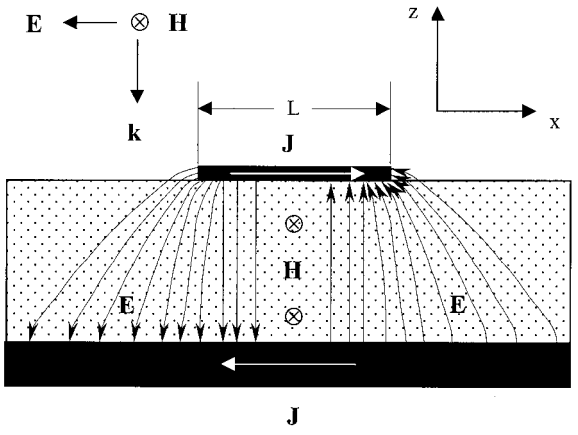

Fig. 1. Side view of a microstrip patch antenna. The patch length is slightly shorter than half the wavelength scaled to the index of refraction of the dielectric substrate. The induced antenna fields and currents are also shown.

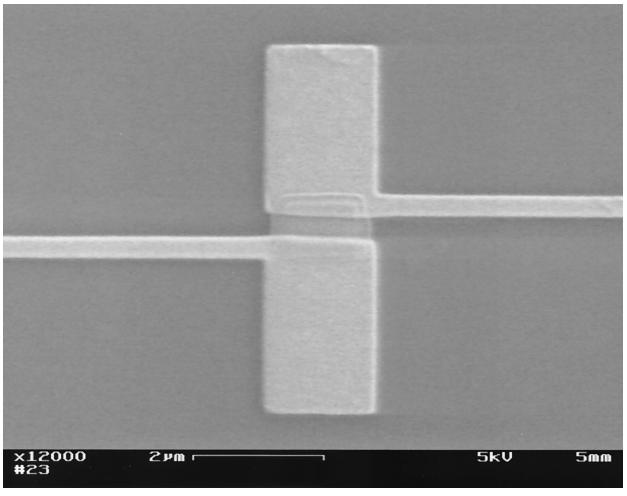

Fig. 2. Electron micrograph of a dipole-antenna-coupled microbolometer.

center of the patch. The microstrip patch antenna converts the incident plane wave with the electric field parallel to the metallic patch into a guided wave with the electric field perpendicular to the metallic patch. However, Fig. 1 shows that close to the edge of the patch the electric field has a small component parallel to the patch. The electric field is not entirely confined within the dielectric substrate, extending partially into the air above. This phenomenon is commonly referred to as fringing. Because of fringing the microstrip patch is electrically longer than its actual physical dimension. This is why the physical length of the patch is chosen to be slightly less than half the dielectric wavelength. At resonance, the *electrical length* of the patch must equal half the dielectric wavelength. The amount of fringing depends on the antenna geometry and on the dielectric permittivity of the substrate. For a given substrate thickness a low dielectric constant allows more fringing than does a high dielectric constant. The fringing of the electric fields is more pronounced in an antenna built on a thicker substrate.

We investigated the use of microstrip antennas for the detection of near 10 μm in wavelength IR radiation.[6,7] Because of the inherent high ohmic and dielectric losses at IR frequencies, the microsensor needs to be incorporated within the antenna volume. One of the simplest integration schemes places the microsensor at the center of the microstrip patch leading to a dipole-antenna-coupled IR detector. The difference between a printed dipole antenna and a microstrip dipole antenna is that the latter incorporates a ground plane. In this paper we study the influence of the dielectric substrate on the performance of microstrip dipole-antenna-coupled microbolometers.

2. Integrated Detector Fabrication

The first step in the fabrication process was to coat the silicon wafer with a nominally 200-nm-thick layer of plasma-enhanced chemical vapor deposition (PECVD) silicon oxide to ensure electrical and thermal insulation between the antenna and the silicon wafer. A finite ground-plane pattern was defined into a 400-nm-thick bilayer of electron-beam resist. After evaporation of 10 nm of titanium and 100 nm of gold, the excess metal was lifted off. The titanium layer provided adhesion between gold and silicon oxide. The antenna dielectric spacer consisted of PECVD silicon dioxide. Figure 2 shows a top view of a microstrip dipole-antenna-coupled microbolometer. The dipole antenna, the dc leads, and the contact pads were fabricated by means of lifting off a nominally 100-nm-thick layer of gold electron-beam evaporated on top of a bilayer of electron-beam resist. The width of the antenna arms was 1.6 μm, and the dc leads were 350 nm wide. Two 300 μm × 200 μm contact pads (not shown in Fig. 2) were placed 40 μm apart. The dc leads connect the antenna to the contact pads. The 1.6 μm × 1.0 μm bolometer was fabricated by means of sputtering a 70-nm-thick layer of niobium on top of a patterned electron-beam resist layer, followed by lift-off. Niobium was chosen as the bolometer material because it has a large bulk electrical resistivity ($1.5 \times 10^{-7}\ \Omega \cdot \mathrm{m}$)[8] and a large temperature coefficient of resistance ($0.005\ \mathrm{K}^{-1}$).[9] The electrical resistivity of the as-deposited niobium thin films is larger than the bulk electrical resistivity. The large electrical resistivity provides a good impedance matching of the microbolometer to the antenna, and the high temperature coefficient of resistance provides a large detector responsivity. Sputtering was employed to deposit niobium because it is more isotropic than evaporation and thus provides better step coverage. The measured electrical resistance of the antenna-coupled detectors was nominally 50 Ω.

3. Measurements and Discussion

The detectors were tested with normally incident, 10.6-μm-wavelength, linearly polarized CO_2 laser radiation. The laser beam was focused by F/1 optics, resulting in an almost diffraction-limited spot with a $1/e^2$ radius of 13 μm and an irradiance of ~1000

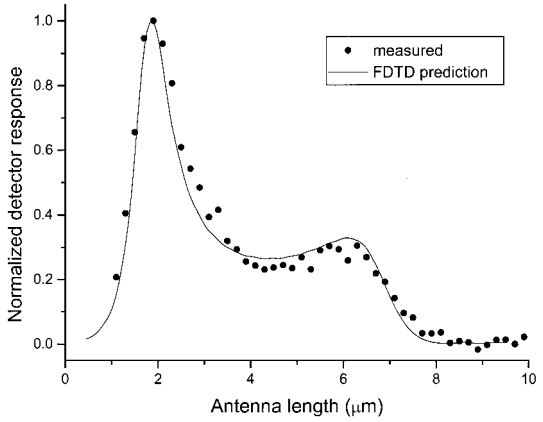

Fig. 3. Normalized detector response versus antenna length for a microstrip dipole-antenna-coupled microbolometer.

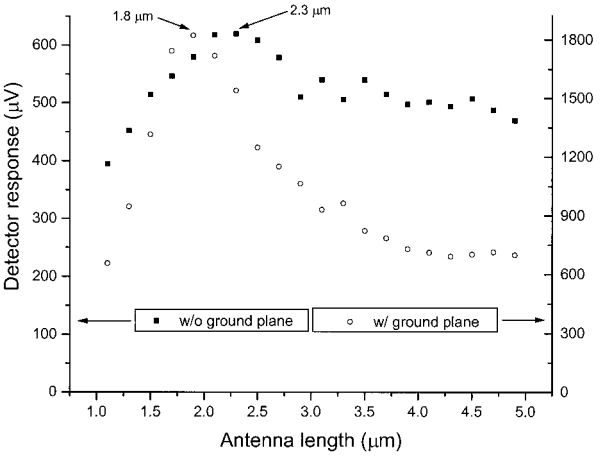

Fig. 4. Influence of the ground plane on the magnitude, position, and width of the antenna resonance.

W/cm^2. Thin aluminum wires bonded to the gold contact pads connect the device to the biasing and readout circuit. The detectors under test were biased at 2 mA and placed in the focus of the laser beam. A mechanical chopper modulated the laser beam at 2.5 kHz, and the change in the voltage across the terminals of the detector was recorded with a lock-in amplifier after a 10× preamplification.

Figure 3 shows the typical response versus dipole full length for a microstrip dipole-antenna-coupled IR detector. The 10.6-μm CO_2 laser radiation was polarized along the antenna arms. The antenna was separated from the finite ground plane by a 550-nm-thick layer of silicon dioxide. The first maximum of the detector response, occurring at 1.8 μm, corresponds to the half-wave antenna resonance, referenced to the dielectric wavelength. The peak at 6.2 μm corresponds to the 3/2-wave antenna resonance. Figure 3 also shows the excellent qualitative agreement between the measured detector response and the squared magnitude of the current induced at the center of the antenna. The induced current was computed using a code developed by the authors based on the three-dimensional finite-difference time-domain (FDTD) method.

Devices without a ground plane, referred to as *printed* dipole-antenna-coupled microbolometers, were also fabricated and tested. The devices were illuminated from the air side. Figure 4 compares the detector response versus antenna length for devices with and without a ground plane. Both types of detectors were fabricated on a 550-nm-thick layer of silicon oxide. The presence of the ground plane shifts the first resonance toward shorter antenna lengths. The ground plane also increases the magnitude of the half-wave resonance because the electromagnetic energy is better confined under the antenna. The response of the detectors with ground plane is three times stronger than the response of the devices without a ground plane. The better confinement of the fields leads to a higher antenna quality factor and thus to a narrower resonance.

Table 1 compares the characteristics of devices separated from the ground plane by oxide layers of different thicknesses. Two mechanisms contribute to the increase of the detector response with the thickness of the oxide layer. First, the gain of the microstrip dipole antenna increases with dielectric thickness. The thicker the dielectric, the more pronounced the fringing of the electromagnetic fields at the edges of the antenna. This allows for a better coupling of the impinging free-space electromagnetic fields into the antenna fields. Second, thicker oxide layers provide better thermal insulation between the microbolometer and the silicon wafer, and therefore more of the dissipated energy is retained in the microbolometer. The gain of a microstrip antenna is not sensitive to the thickness of the dielectric substrate, especially for substrates with low dielectric constant.[5] Therefore the detector response increases with the thickness of the substrate mainly because of the better thermal insulation provided by a thicker substrate. Better thermal insulation also leads to slower detector response. The location of the first resonance shifts toward shorter dipoles as the oxide thickness increases. The fringing of the antenna fields also explains this shift, because a microstrip dipole of a certain length printed on a thicker dielectric layer is longer from an electrical viewpoint.

The effect of the dielectric substrate on the detector response was further investigated by incorporation of an air layer between two oxide layers. After the finite ground plane was defined, a 120-nm-thick layer of oxide was deposited by PECVD at 275 °C. This layer was deposited to ensure that enough material is

Table 1. Characteristics of Devices with Different Oxide Thicknesses

Wafer	Oxide Thickness (nm)	V_{max} (μV)	Peak Location (μm)	Time Constant (ns)
1	190	265	1.9	170
2	550	1925	1.8	390
3	900	3845	1.6	1190

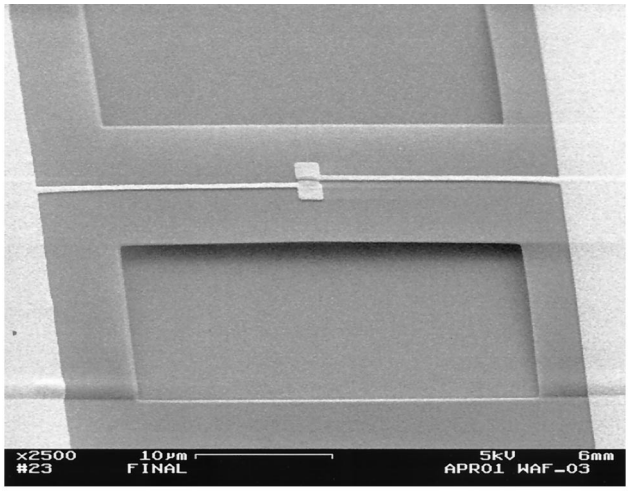

(a)

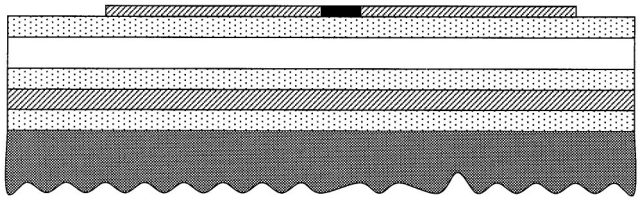

(a)

Fig. 5. Microstrip dipole antenna with sandwiched substrate: (a) electron micrograph, (b) side-view schematic. Nb, niobium; Au, gold; SiO_2, silicon dioxide; Si, silicon.

present between the bond pads and the ground plane during the device packaging process. If the oxide layer between the contact pads and the ground plane is too thin, the pressure applied during the wire-bonding process may bring the bond wires in contact with the ground plane, thus shorting out the device. A 220-nm-thick layer of negative resist (NEB-31) was then spun on top of the oxide layer and patterned by electron-beam lithography. A second layer of oxide (160 nm thick) was then deposited by PECVD at 150 °C. After the antenna and the microbolometer were fabricated, windows were opened into the top oxide layer by reactive ion etching. The resist between the two oxide layers was removed by use of oxygen plasma in a barrel etcher. Figure 5(a) shows an electron micrograph of the device after the NEB layer was etched with the oxygen plasma. A schematic side view of a device with sandwiched substrate is shown in Fig. 5(b). The top oxide layer provides physical support for the antenna and the dc leads.

Figure 6 compares the detector response versus antenna length for devices separated from the ground plane by a homogeneous layer of oxide and devices incorporating an air layer into the dielectric spacer. The distance between the antenna and the ground was nominally 500 nm in both types of detectors. The solid curves represent the predicted detector response by the FDTD method. The locations of the antenna resonances shift toward longer dipoles when

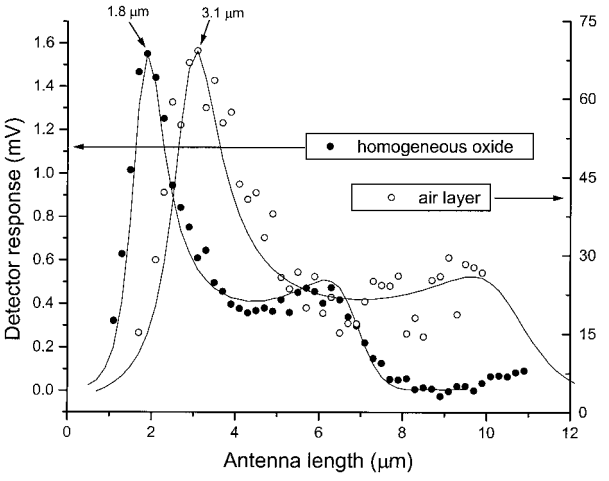

Fig. 6. Detector response versus antenna length. Devices with homogeneous dielectric substrate compared with devices incorporating an air layer within the substrate.

the air layer is included between the oxide layers. At the same time, the bandwidth of the first resonance is widened because the effective dielectric constant of the dielectric spacer is reduced. The air layer provides better thermal insulation between the antenna and the silicon wafer. The responsivity of the devices with sandwiched substrate is 45 times larger than the responsivity of the devices with oxide substrate. Figure 7 shows the normalized detector response as a function of the modulation frequency of the laser beam. The laser beam was modulated with an acousto-optic modulator. As expected from the responsivity data,[9] the devices with the air layer incorporated into the dielectric substrate are a corresponding factor of 45 times slower than the devices with homogeneous oxide substrate.

Silicon oxide is widely used in the integrated circuit technology. It was chosen as antenna dielectric substrate because it was readily available in the fabrication process. However, it absorbs IR radiation.[10]

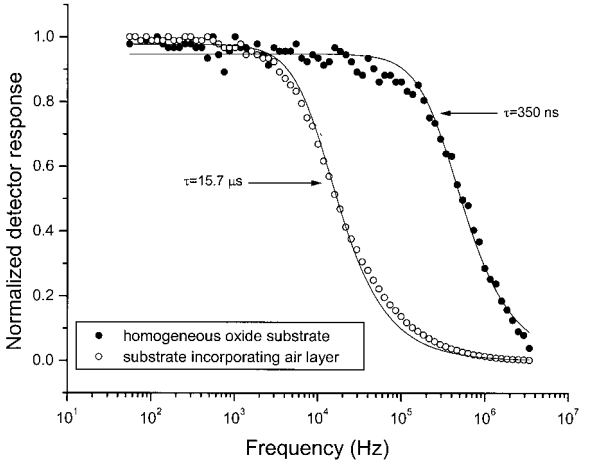

Fig. 7. Normalized detector response versus the modulation frequency of the laser beam.

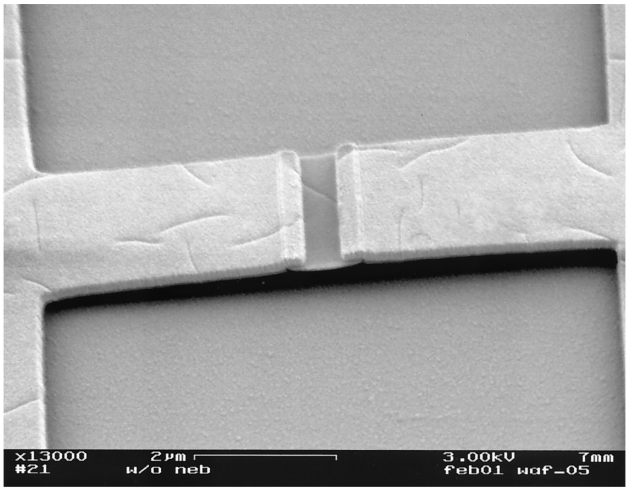

(a)

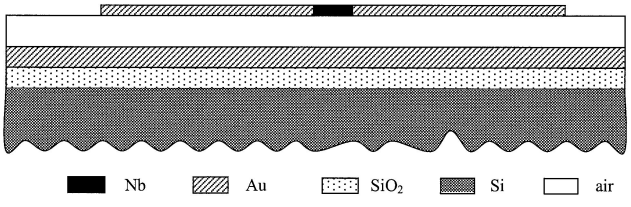

(b)

Fig. 8. Bridge microstrip dipole-antenna-coupled microbolometer: (a) electron micrograph, (b) side-view schematic. Nb, niobium; Au, gold; SiO_2, silicon dioxide; Si, silicon.

We reported on the effect of the dielectric losses on the performance of microstrip antenna coupled microbolometers.[7] To eliminate absorption within the dielectric substrate, bridge dipoles were fabricated. Figure 8 shows a microstrip dipole antenna suspended above the ground plane. To ensure mechanical stability, the dipole was connected directly to the contact pads. A 500-nm-thick layer of NEB-31 was spun on top of a 100-nm-thick, finite (30 μm × 30 μm) ground plane. The NEB layer was patterned into a square (40 μm × 40 μm) post aligned with the finite ground. A rectangular (1.0 μm × 2.0 μm) microbolometer pattern was defined into a bilayer of electron-beam resist spun on top of the NEB layer. A 40-nm-thick layer of titanium was electron-beam evaporated, and the excess metal was lifted off. The antenna and the contact pads pattern, defined into a bilayer of electron-beam resist, was aligned with the titanium microbolometer. After the evaporation and lift-off of the antenna metal (200-nm-thick gold layer), an oxygen plasma isotropic etch was used to remove the NEB from under the bridge dipole.

The measured detector response versus antenna length is shown in Fig. 9 along with the FDTD prediction. Both the thermal insulation of the microbolometer from the silicon wafer and the antenna gain are improved by elimination of the silicon oxide antenna substrate. However, the dipole antenna provides a low-thermal-impedance path from the microbolometer to the contact pads. As a result the

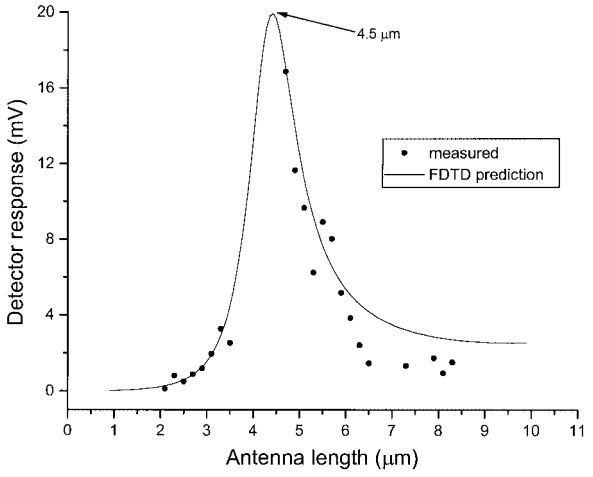

Fig. 9. Detector response versus antenna length for a bridge microstrip dipole-antenna-coupled microbolometer.

maximum detector response for a bridge dipole is lower than the maximum response of a microbolometer integrated with a dipole antenna with an air layer within its dielectric substrate. The half-wave resonance of a dipole antenna separated from the ground plane by a 500-nm-thick layer of silicon dioxide occurs at 1.8-μm antenna length, as seen in Fig. 6. Eliminating the oxide between the antenna and the ground plane shifts the resonant length to 4.5 μm. The bridge microstrip dipole design relaxes the lithographic requirements because the lower dielectric constant lengthens the dielectric wavelength. Hence a structure of given dimension will resonate at a shorter free-space wavelength when fabricated in an air bridge configuration.

4. Conclusions

We have investigated the effect of the dielectric substrate on the performance of microstrip antenna-coupled microbolometers. The ground plane shifts the position of the antenna resonance toward shorter dipoles. In the presence of the ground plane the magnitude of the antenna resonance increases and its width decreases. The presence of the ground plane leads to a better confinement of the electromagnetic energy within the antenna substrate and thus to a higher Q factor.

Devices with thicker dielectric substrates had higher responsivity and longer time constants. A thicker substrate provides better thermal insulation between the antenna and the silicon wafer. The gain of a microstrip dipole antenna increases with the thickness of the dielectric substrate. The position of the antenna resonance shifted toward shorter antennas as the thickness of the dielectric substrate increased. Thicker substrates allow more extended fringing fields and from an electric point of view the antenna looks longer.

The position of the antenna resonance shifted toward longer dipoles when an air layer was incorporated within the antenna substrate, because the

effective dielectric constant of the substrate was decreased. The magnitude of the detector response increased as a result of better thermal insulation between the antenna and the silicon wafer. Bridge dipoles were fabricated to eliminate absorption within the antenna dielectric substrate. As expected, the position of the antenna resonance shifted toward longer dipoles. When shifting the resonance is shifted to longer antennas, the bridge dipole design relaxes the lithographic requirements. This opens the possibility of using step-and-repeat optical lithography techniques for the fabrication of antenna-coupled IR detectors.

This material is based upon research supported by NASA grant NAG5–10308.

References

1. S. Y. Wang, T. Izawa, and T. K. Gustafson, "Coupling characteristics of thin-film metal-oxide-metal diodes at 10.6 μm," Appl. Phys. Lett. **27,** 275–279 (1975).
2. C. Fumeaux, M. A. Gritz, I. Codreanu, W. L. Schaich, F. J. Gonzalez, and G. D. Boreman, "Measurement of the resonant lengths of infrared dipole antennas," Infrared Phys. Technol. **41,** 271–281 (2000).
3. N. Chong and H. Ahmed, "Antenna-coupled polycrystalline silicon air-bridge thermal detector for mid-infrared radiation," Appl. Phys. Lett. **71,** 1607–1609 (1997).
4. E. N. Grossman, J. E. Sauvageau, and D. G. McDonald, "Lithographic spiral antennas at short wavelengths," Appl. Phys. Lett. **59,** 3225–3227 (1991).
5. C. A. Balanis, *Antenna Theory: Analysis and Design* (Wiley, New York, 1997).
6. I. Codreanu, C. Fumeaux, D. F. Spencer, and G. D. Boreman, "Microstrip antenna-coupled infrared detector," Electron. Lett. **35,** 2166–2167 (1999).
7. I. Codreanu and G. D. Boreman, "Infrared microstrip dipole antennas—FDTD predictions versus experiment," Microwave Opt. Technol. Lett. **29,** 381–383 (2001).
8. D. R. Lide and H. P. R. Frederiske, eds., *CRC Handbook of Chemistry and Physics* (CRC Press, Boca Raton, Fla., 1996).
9. E. L. Dereniak and G. D. Boreman, *Infrared Detectors and Systems* (Wiley, New York, 1996).
10. H. R. Philipp, "Silicon dioxide (SiO_2) (Glass)," in *Handbook of Optical Constants of Solids*, E. D. Palik, ed. (Academic, New York, 1985), pp. 749–763.